

AD-A115 938

CALIFORNIA UNIV SANTA BARBARA QUANTUM INST

F/O 20/7

THREE DIMENSIONAL RADIATION FIELDS IN FREE ELECTRON LASERS USIN--ETC(U)

OCT 81 L R ELIAS, J GALLARDO

N00014-80-C-0308

UNCLASSIFIED

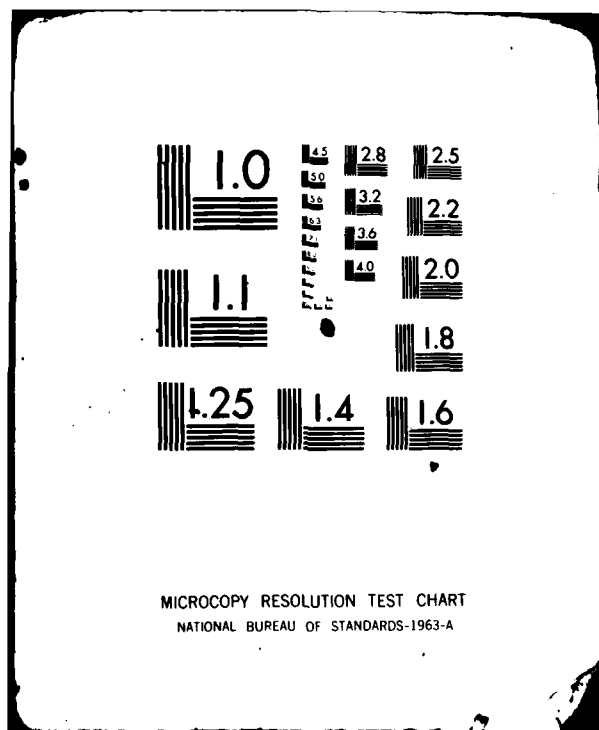
01FEL-012/81

AM

1-1
2-1

1





AD A115938

395-202 Logged
10/1/81 OA

Log & File
Contracts
reports

①

Three Dimensional Radiation Fields
in Free Electron Lasers Using
Lienard-Wiechert Fields

by Luis R. Elias and Juan Gallardo
Quantum Institute
University of California at Santa Barbara 93106
QIFEL012/81

OCTOBER 28, 1981

UNIVERSITY OF CALIFORNIA
SANTA BARBARA
QUANTUM INSTITUTE
FREE ELECTRON LASER PROJECT

DTIC FILE COPY



DTIC
ELECTE
JUN 22 1982
S B D

DISTRIBUTION STATEMENT A

Approved for public release;
Distribution Unlimited

82 05 25 03

Three Dimensional Radiation Fields in
Free Electron Lasers Using
Lienard-Wiechert Fields

Luis R. Elias and Juan Gallardo
The Quantum Institute
University of California at Santa Barbara 93106


Research supported by The Office Of Naval Research and Air
Force Office of Scientific Research, Contract
N00014-80-C-0308

INTRODUCTION

In a free electron laser a relativistic electron beam is bunched under the action of the ponderomotive potential and is forced to radiate in close phase with the input wave. Until recently, most theories of the FEL have dealt solely with electron beams of infinite transverse dimension radiating only one-dimensional E.M. waves (plane waves).¹ Although these theories describe accurately the dynamics of the electrons during the FEL interaction process, neither the three dimensional nature of the radiated fields nor its non-monochromatic features can be properly studied by them. As a result of this, very important practical issues such as the gain per gaussian-spherical optical mode in a free electron laser have not been well addressed, except through

For	<input checked="" type="checkbox"/>
I	<input type="checkbox"/>
d	<input type="checkbox"/>
ion	<input type="checkbox"/>
PER LETTER	
on/	
ity Codes	
avail and/or	
Special	
Dist	
A	




a one dimensional field model in which a filling factor describes crudely the coupling of the FEL induced field to the input field. 

In an effort to alleviate this problem a computer code is presently under development at UCSB to study the three-dimensional characteristics of fields radiated by FELs. It is based on the coherent superposition of electromagnetic pulses radiated by individual electrons in the beam. The three dimensional fields of each pulse of radiation is calculated numerically from the Lienard-Wiechert solutions to the wave equation. Included in these calculations are the effects of the FEL ponderomotive force on the motion of the electron. Other approaches to solve the 3D FEL problem are also presently under development.^{2,3,4,5}

In this paper, some preliminary numerical calculations of the angular and spectral characteristics of the radiated field of a constant period FEL is presented. Although the work is mostly numerical in nature, the approach used (i.e. single particle radiation fields) gives good understanding of the physics of the FEL wave-beam interaction process.

The most notable results presented here can be summarized as follows: Although individual electron radiation pulses carry information of relatively large spectral bandwidth and relatively large angular distribution



patterns, because of the bunching of the electron beam by the ponderomotive forces, the coherent superposition of radiation pulses from all electrons in the beam produce, as a result of wave interference effects, a narrower cone of radiation and a more monochromatic radiation pulse than the corresponding effects expected from a single electron. It is found that FELs can produce a pulse of radiation whose half-angle at half-power is approximately given by $1/N$, where N is the number of periods in the magnetic wiggler and whose bandwidth (for long electron pulse lengths) is approximately given by $1/\Delta t$, where Δt is the duration of the electron pulses.

THE LIENARD-WIECHERT FIELDS AND EQUATION OF MOTION

The retarded solution of the wave equation for an accelerated point-charge particle moving with relativistic energy γmc^2 is given by the well know Lienard-Wiechert fields⁶

$$\vec{E}(\vec{x}, t) = \frac{q}{4\pi\epsilon_0} \left[\frac{\vec{R} - \vec{R}\vec{\beta}}{\gamma^2 (\vec{R} - \vec{R}\vec{\beta})^3} + \frac{1}{c} \frac{\vec{R} \times (\vec{R} - \vec{R}\vec{\beta}) \times \dot{\vec{\beta}}}{(\vec{R} - \vec{R}\vec{\beta})^3} \right]_{\text{RET}} \quad (1)$$

and

$$\vec{B} = \frac{\vec{R} \times \vec{E}}{Rc} \quad (2)$$

where the fields are evaluated at the observation position \vec{x} at the time t . The quantities \vec{R} , $\vec{\beta}$ and $\dot{\vec{\beta}}$ are respectively the radius vector from the particle to the observation point, the instantaneous normalized velocity vector and acceleration vector of the particle. All quantities inside the brackets must be evaluated at the retarded time t' defined by the following relation

$$t = t' + \frac{|\vec{R}(t')|}{c} \quad (3)$$

The first term in equation (1) describes the Coulomb field of a moving particle. The second term describes its radiation field. The motion of the particle is governed by the Lorentz force equation

$$\frac{d\vec{p}}{dt} = q \left[\vec{E} + \vec{v} \times \vec{B} \right] \quad (4)$$

It can be shown⁸ that the transverse motions of the electron in a free-electron laser is determined with good accuracy by the wiggler field B_w alone. The longitudinal motion of the electron, on the other hand, is governed by the ponderomotive force. For a helical wiggler and a circularly polarized

input plane wave the force is given by:

$$\frac{dp_z}{dt} = qc \frac{K}{\gamma} E_s \sin \psi \quad (5)$$

$$\psi = k_0 z + kz - \omega t \quad (6)$$

where $K = q\lambda_0 B_w / 2\pi mc$, and λ_0 is the period of the wiggler. E_s is the amplitude of the input plane wave. Equations (5) and (6) can be solved numerically for the position z of the particle. Using this result and equation (3), \vec{E} and \vec{B} can be then evaluated at \vec{x} at time t .

RADIATION FROM A SINGLE ELECTRON

The three dimensional radiation fields from a single electron moving solely under the influence of a constant period wiggler has been studied in detail.⁷ Radiation reaction forces are small and do not affect the motion of the electron as it radiates. At an angle of observation θ with respect to the axis of motion an observer far away from the wiggler will see coming a pulse of radiation N periods long, of approximate constant amplitude and phase. The wavelength

of the radiation field for a helical wiggler is given by

$$\lambda = \frac{\lambda_0}{2\gamma^2} [1 + (\gamma\theta)^2 + K^2] \quad (7)$$

For small wiggler fields the radiation can be shown to have an angular half-angle width $\theta_s \approx 1/\gamma$ approximately. Also, it can be shown that again for small wiggler field most of the energy is radiated within a narrow band of wavelength given very nearly by

$$\frac{\Delta\lambda}{\lambda} \approx \frac{1}{2N} \quad (8)$$

where N is the number of periods in the wiggler. A typical radiation pulse from an electron moving in a magnetic wiggler is shown by the broken line in figure 1. Note that amplitude and phase remains very nearly constant with time. The amplitude of the radiation field is proportional to the maximum transverse accelerations given to the electron by the magnetic wiggler. Since the maximum acceleration of the electron does not vary with positions along the magnet, then the radiated pulse amplitude will not change with time. Also, the phase of the wave remains constant because the wiggler periodicity is constant and the average longitudinal velocity of the electron remains constant (i.e. there is no

ponderomotive force).

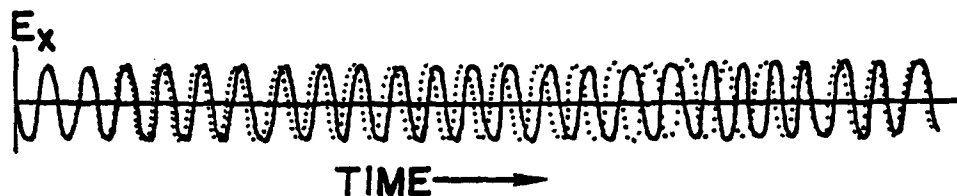


Figure 1. The broken line represents a typical radiation field emitted by an electron in a wiggler. The solid line represents the input plane wave. Both fields were observed at a fixed point in space.

In an FEL the radiation pulse emitted by an electron is different from that of a single electron in a wiggler alone. As will be shown below the ponderomotive force affects mainly the phase of the radiated field. The geometrical arrangement is illustrated in figure 2.

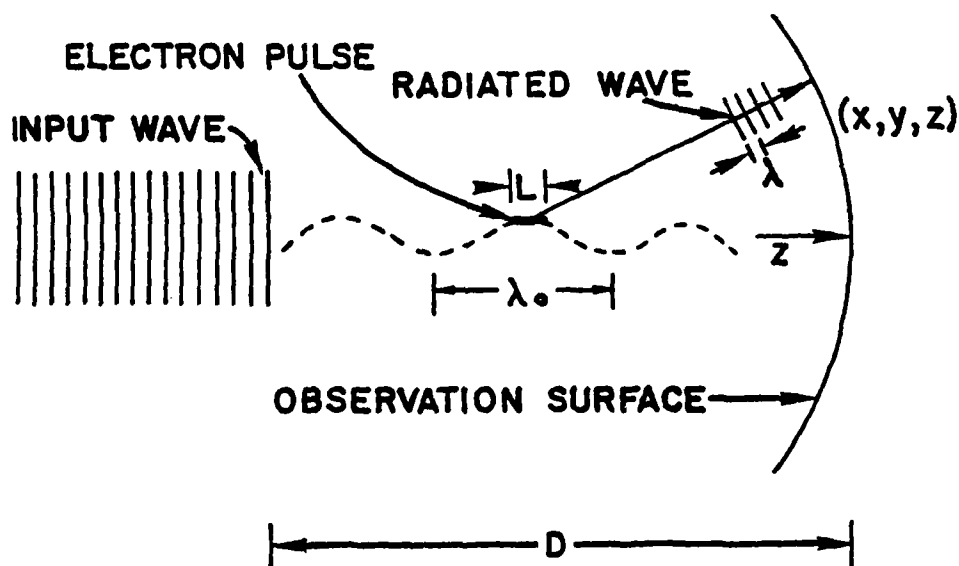


Figure 2. Geometrical arrangement corresponding to an FEL amplifier configuration.

It can be easily shown that for practical FELs the longitudinal acceleration of the electron under the influence of the ponderomotive force is much smaller than the transverse acceleration of the electron provided by the magnetic wiggler.

$$\frac{|\dot{\beta}_z|}{|\dot{\beta}_\perp|} \approx \frac{qE_s \lambda}{\gamma m c^2 \pi} \quad (9)$$

The above ratio can be interpreted as the ratio of the energy radiated by the electron in one optical wavelength to the total energy of the electron. Even at an optical power density where gain-saturation begin to occur the above relation gives

$$\frac{|\dot{\beta}_z|}{|\dot{\beta}_\perp|} \approx \frac{1}{4\pi(\gamma N)^2} \quad (10)$$

For example if $N=20$ and $\gamma=7$ then the above ratio yields $|\dot{\beta}_z|/|\dot{\beta}_\perp| \approx 4 \times 10^{-6}$. The above values of γ and N are the ones used to obtain the results presented in this paper. As a result of the above calculation, the longitudinal acceleration term produced by the ponderomotive force in a FEL does not contribute significantly to the amplitude of the radiated field and has thus not been included in these calculations. However, as it is indicated in figure 1 by the

broken line, the effect of the ponderomotive force is to change the longitudinal position of the electron and thus change the phase of the radiated wave as shown in the figure. In other words, the ponderomotive force affects equation (3) to a much greater extent than it affects equation (1).

RADIATION FROM A BEAM OF ELECTRONS IN A WIGGLER

If there is no ponderomotive force, the radiation fields produced by a beam of electrons moving along a magnetic wiggler will depend on the way the charge is distributed along the beam. For example, if the electron beam contains a uniform longitudinal charge distribution then, due to the uniform distribution of phases of the individually radiated pulses, the resultant radiation fields will be exactly zero. For this situation only static electromagnetic fields can be present. If, on the other hand, the longitudinal charge distribution in the beam is random, then the distribution in phases of the individual radiation pulses will be also random. As a result of this, there will be a finite resultant fluctuating radiation field with mean amplitude proportional to $\sqrt{N_e}$, where N_e is the number of electrons that radiate pulses which can interfere simultaneously at a fixed point in space. The radiation fields produced will have on

the average the angular and spatial radiation characteristics of that of a single electron as discussed in the previous section.

If the ponderomotive FEL force is present, then the radiation characteristics of the electron beam can be drastically different from that of a single particle. The amplitude of the resultant radiated field can be forced to be proportional to N_e , rather than to $\sqrt{N_e}$ for random distribution of phases, as a result of the bunching effects produced by the ponderomotive force. This is the basic mechanism by which free electron lasers work.

RESULTS OBTAINED

In this section, a summary is presented of the numerical analysis of the three dimensional fields radiated by a constant period free-electron laser. In figure 2 is illustrated the geometrical arrangement. L is the electron pulse length of the filamentary beam shown as a heavy dark line. λ_0 is the magnetic helical wiggler periodicity. The distance between the spherical surface of observation and the entrance to the wiggler is D . The observation point is located at (x,y,z) . Table I below summarizes some of the FEL interaction parameters used.

TABLE 1.

Magnetic wiggler period (λ_0)	2cm
Amplitude of magnetic field (Bw)	0.05T
Input wave wavelength (λ)	200 μ m
Input wave optical power density	10 ⁷ watts/cm ²
Number of magnet periods	20
Electron energy (γ)	7

The following restrictions were imposed on the calculations: a) no interaction between electrons were allowed, b) the input wave field and the wiggler fields were represented by plane waves, c) the electron trajectories were solely determined by the magnetic wiggler force, d) no radiation reaction forces were included to calculate the radiation fields produced by each electron and e) no changes in amplitude or phase of the input signal were taken into consideration (low gain conditions).

All of the results presented here pertain to the radiation fields produced by the electrons alone. In order to calculate such things as laser gain the radiated fields will have to be summed coherently to the input field.

Figure 3 shows typical time-records of one of the components of the radiated field produced by a beam of

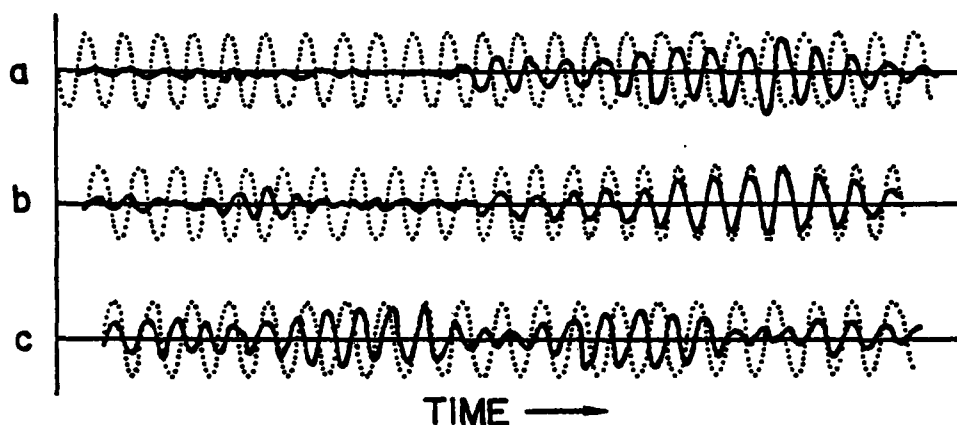


Figure 3. Time record of the x-component of the radiated electric field on axis (a) $\beta_z = \beta_R^z$, (b) $\beta_z > \beta_R^z$, and (c) $\beta_z > \beta_R^z$.

The dotted line represents the x-component of the electric field of the input monochromatic wave.

electrons of length $L=10\lambda$ as observed on axis at the point $(0,0,5m)$. The dotted lines represent the phase information of the input wave (gaussian TEM₀₀) and the solid curves represent the radiated field. Figure 3a shows the radiation field observed for a pulse of electrons injected with initial velocity equal to the resonance velocity

$$\beta_R^z = \frac{\lambda_0}{\lambda_0 + \lambda} \quad (11)$$

Initially, due to the uniform distribution of charge in the electron pulse, there is field cancellation. As the electron beam becomes bunched by the ponderomotive force there is a

finite growth of the radiated field. Very nearly at the end of the time record the beam has achieved maximum bunching and consequently the amplitude of the radiated field has reached its maximum value also. Note that at resonance the resultant radiated wave is out of phase by $\pi/2$ with respect to the input wave. If added to the input wave the radiation field will not change the amplitude of the input wave (i.e. no signal gain occurs). This can be easily shown by adding two waves of the same frequency but different amplitude and phase. If the restriction is imposed that the resultant amplitude be equal to the amplitude of one of the input waves the following relation must hold:

$$\tan \phi = -\frac{A}{2B} \quad (12)$$

where A is the amplitude of both the input wave and the resultant wave, B is the amplitude of the second input wave, and ϕ is the phase difference that must exist between the two input waves. For the case in question $B/A \rightarrow 0$ (low gain condition). Thus $\phi \rightarrow \pi/2$ as observed in the time record of figure 3a.

The results shown in figure 3b represent the radiated wave by the same pulse of electron as in figure 3a but with initial longitudinal velocity $\beta_z > \beta_R^z$. In fact, the initial

velocity was chosen to correspond with that for maximum average electron energy deceleration (i.e. at the peak of the one-dimensional gain curve). It can be seen from figure 3b that the radiated wave now has the same phase as the input wave. Thus, net amplification of the input wave is possible. Similarly, for $\beta_z < \beta_R^z$ a net absorption of the input wave can occur ($\phi \approx \pi$). In figure 3c the radiated pulse shown was produced by the same electron pulse but with initial $\beta_z \gg \beta_R$. The phase of the radiated wave is now oscillating in time. If added to the input wave the resultant wave will have the same amplitude as the input wave. The phase oscillation of the radiated wave can be explained by the fact that although the bunching of the electron beam occurs with a spatial periodicity close to that of the input wave wavelength the electrons radiate individually at shorter wavelengths because $\beta_z \gg \beta_R^z$. Thus, a beating effect appears.

To compare the results obtained above with results obtained in one dimensional FEL theories, a series of computer runs were made to determine the actual optical gain curve on axis as a function of input electron beam velocity. The radiated field was calculated on axis and added to the input-field (a plane wave) evaluated on axis. The on-axis gain was thus calculated and shown (see figure 4) to have the same form as that predicted by one dimensional theories and

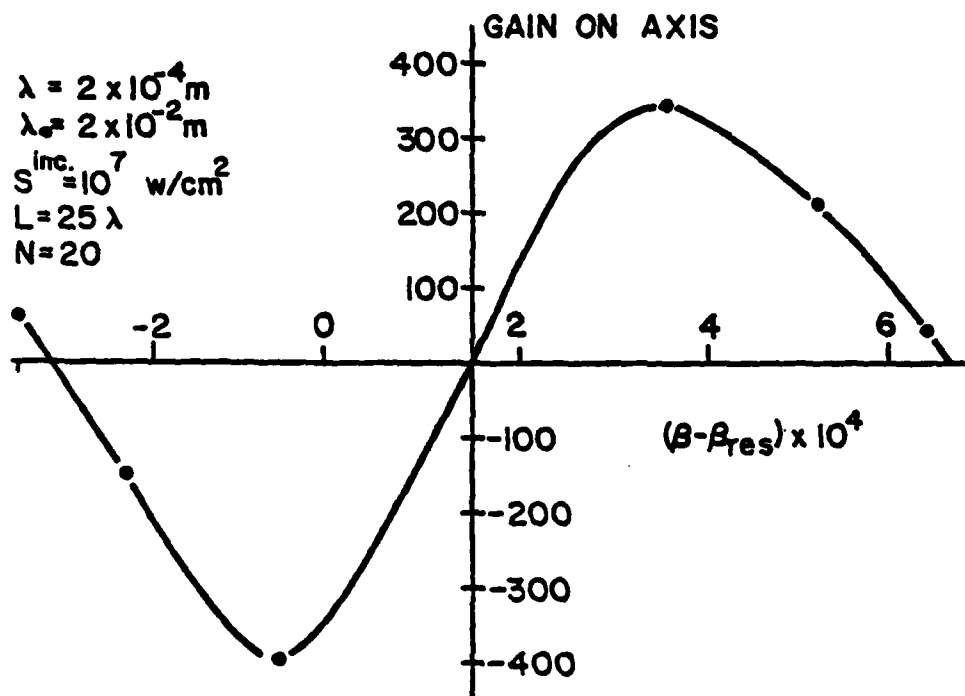


Figure 4. Optical gain on axis as a function of initial longitudinal velocity.

that obtained experimentally by the Stanford group. However, one important difference can be noted immediately between the two results. The 3D optical gain curve on axis is shifted by an amount $\delta\beta_z$ toward larger initial velocity with respect to the 1D gain curve. The 3D results showed that the radiated wave was in phase ($\phi=0$) with the input plane wave at the point of observation. This is not in contradiction with the results shown in figure 3 because the latter were obtained with an input gaussian TEM₀₀ wave. The phase of the TEM₀₀ mode shifts by $\phi=90^\circ$ far away from its waist. Thus, at

resonance the radiated wave has a phase of 90° with respect to the input gaussian wave.

The phase of the radiated wave is therefore very important in determining its coupling strength to the input signal. Calculations of gain for input TEM₀₀ signals will be presented in a later publication.

ANGULAR RADIATION CHARACTERISTICS.

The plots shown in figure 5 illustrate the angular characteristics of radiation in a free-electron laser. Curve 5a describes the angular pattern of radiation for an electron pulse injected with resonant velocity ($\beta_z = \beta_R$) and of very short length $L = \lambda$. The result shown in the figure is what is expected from a single radiating particle. This was discussed earlier ($\theta \approx 1/\gamma$) and confirms the fact that when no coherent effects are present the single particle radiation characteristic dominate. The results shown in figure 5b were obtained with an electron pulse of length $L = 50\lambda$ and with initial resonant velocity ($\beta_z = \beta_R$). It shows how interference effects reduce the solid angle into which energy is radiated. The half-power half-angle shown is nearly 35 mrad compared to 60 mrad for the short pulse. It is possible to think of the resultant radiation as being generated by a long line of phased-array antennas radiating each short pulses of radiation N periods long. From simple grating diffraction theory it

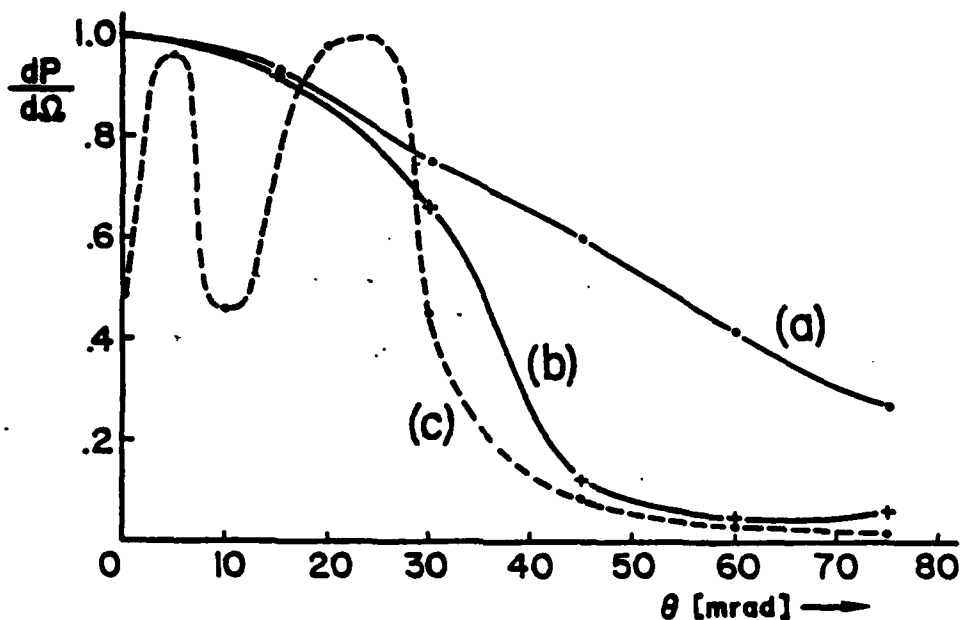


Figure 5. Angular dependence of the radiation of a single filament. a) Very short electron pulse $L=\lambda$ at resonance velocity; b) Long electron pulse $L=50\lambda$ at resonance velocity; c) same electron pulse injected with initial velocity $\beta_z > \beta_R$.

can be shown that radiation will be emitted into a cone of angular dimension given approximately by $1/N_0$ where N_0 is the number of radiators in the antenna. For the FEL, however, N_0 represents the number of electron bunches that can interfere simultaneously at a fixed point in space. After some thought it can be shown that $N_0=N$ for the FEL. That is to say, only N optical periods can interfere simultaneously in the FEL, where N is the number of periods in the wiggler. Figure 5c shows the angular distribution of radiation from a beam injected with energy greater than resonance energy. In fact

β_z was chosen to maximize gain as calculated from the one dimensional theory. The figure shows an interesting ring pattern in the angular distribution of radiation. This can be explained as follows: since the wavelength of radiation is now shorter than that of bunching, it is not possible to add constructively the radiated waves along the beam axis. However, at small angles of observation it should be possible to satisfy the grating relation

$$n\lambda_{\text{RAD}} = \lambda_{\text{BUNCH}} \cos \theta \quad (13)$$

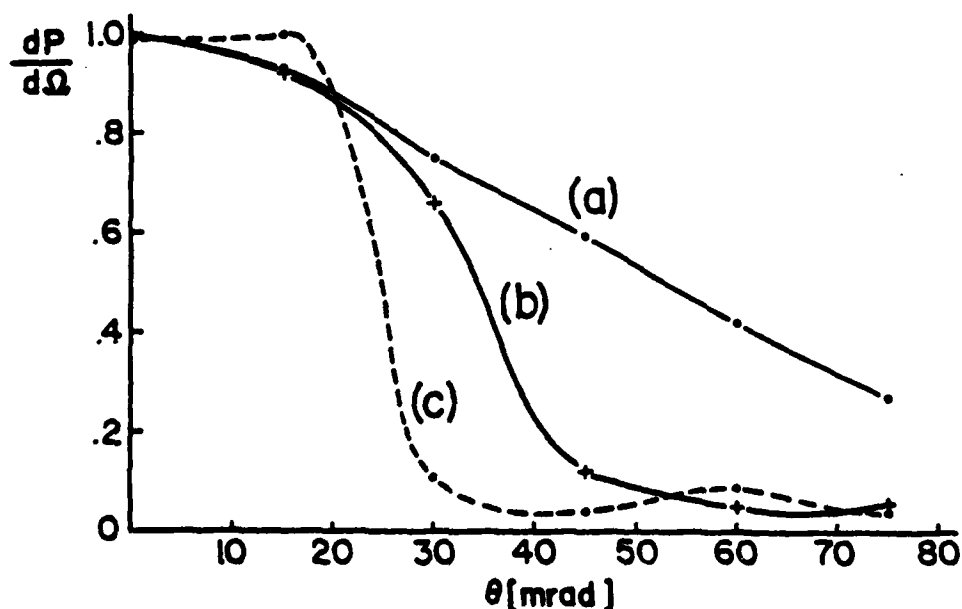


Figure 6. Angular dependence of the radiation of a single filament. a) Very short electron pulse $L=\lambda$ at resonance velocity; b) long electron pulse $L=50\lambda$ at resonance velocity; c) same electron pulse injected with initial velocity $\beta_z < \beta_R$.

where n is the order for constructive interference. Thus, it appears that an electron beam prepared with the energy necessary to give a maximum one-dimensionally calculated optical gain will in fact have lower gain along the axis of the beam. It seems from figure 5c that for $\beta^z > \beta_R^z$ the radiated energy best couples to modes of higher order than that of the TEM₀₀ mode. In figure 6c the energy of the electron pulse ($L=50 \lambda$) was chosen to be below the resonant energy ($\beta_z \leq \beta_z^R$). Here $\lambda_{\text{RAD}} > \lambda_{\text{BUNCH}}$, and as a result there is no angle θ for which the grating formula in equation (13) can be satisfied. Thus, there is no ring structure in the radiation cone.

Figure 7 shows the angular distribution of radiation for a multifilamentary beam injected into the FEL with initial longitudinal velocity $\beta^z = \beta_R^z$. One filament is located on axis and 10 filaments were located over a radius of 2mm. All the radiation waves were summed coherently. The resulting angular radiation cone is smaller than the ones shown in figures 5 and 6. These additional interference effects are not expected to be seen in a real experiment because of the random distribution of electrons in the beam. Since there is no radial bunching force, the radiation fields emitted by electrons from different transverse positions in the beam should be summed incoherently.

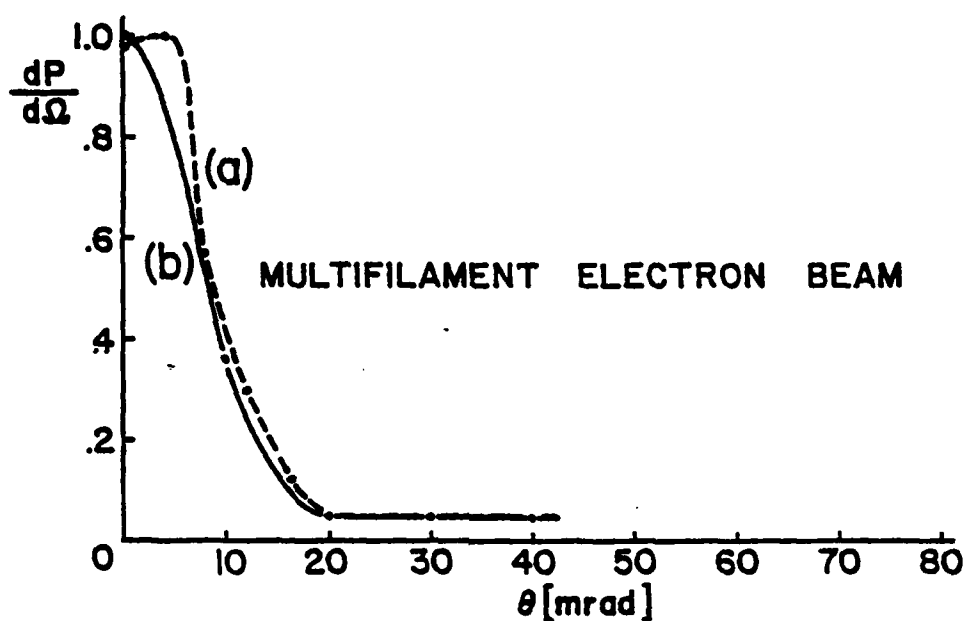


Figure 7. Angular dependence of the radiation from a multifilamentary beam a) $\beta_z < \beta_R^z$; b) $\beta_z > \beta_R^z$.

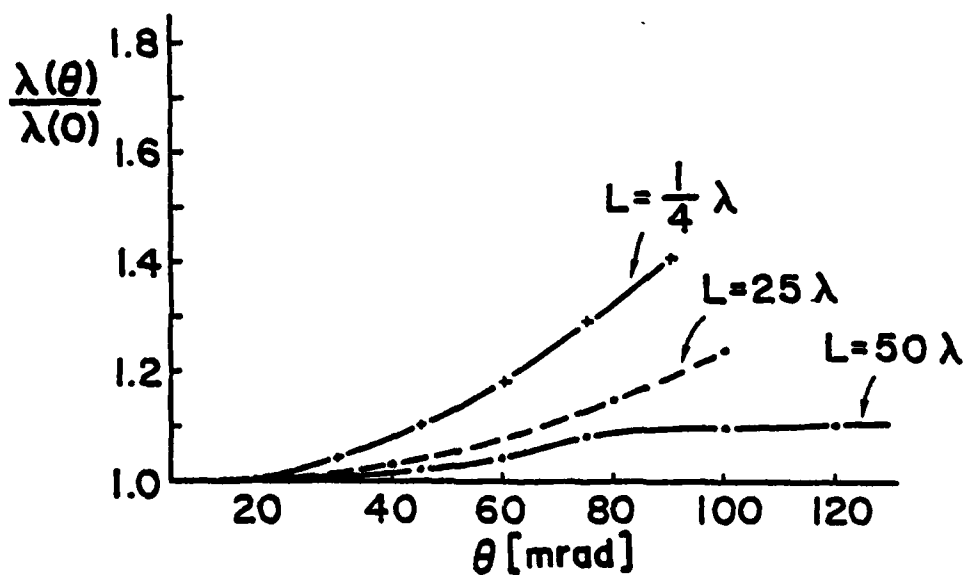


Figure 8. Angular dependence of the radiated wavelength for electron pulses of various lengths.

SPECTRAL RADIATION CHARACTERISTICS

The same interference effects that caused the FEL to radiate into a cone of smaller angle than that of a single electron are evident in the radiated spectrum. In figure 8 the dependence of radiated wavelength with angle is shown for beams of different length injected with the same initial resonant energy. It can be clearly seen that as the number of radiating bunches in the beam increases the bandwidth of radiated energy decreases. That is to say, it is possible to put together a string of radiated pulses and make the resultant pulse more monochromatic (i.e. longer) than any single individual pulse. Thus, the radiation emitted by an electron beam in a FEL is monochromatic by virtue of the temporal interference effects that take place. It is worth noting that for short electron pulses $L=\lambda/4$ the radiated wavelength follows closely the curve for a single electron (e.g. equation 7.)

CONCLUSIONS

Results have been presented that describe the angular and spectral radiation characteristics from a constant period FEL using the Lienard-Wiechert fields. Interference effects determine the angular and spatial characteristics of the radiated field. The radiated spectrum has been shown to be

more monochromatic and concentrated in a smaller radiation cone than that for a single electron.

There is sufficient amplitude and phase information in the radiated field calculations to enable a correct evaluation of the coupling of the radiated field to the input field. Results of these calculations will be presented in a later paper.

The present computer code will be shortly modified to include interactions between electrons. In this way, space charge effects and radiation effects will be calculated in a self-consistent manner to permit calculations of three-dimensional radiation fields in the high gain regime.

REFERENCES

1. "Free-Electron Generators of Coherent Radiation", Physics of Quantum Electronics, Vol. 7 (1980).
2. "The Three-Dimensional Non-linear Theory of the Free Electron Laser Amplifier", P. Sprangle and Cha-Mei Tang, ONR Workshop on FEL, Sun Valley, ID, June 22-25, 1981; NRL Memo Report 4280 (1980), same authors.
3. "Two Dimensional Numerical Model of a Free Electron Laser Amplifier", D. Prosnitz, R.A. Haus, S. Doss and R.J. Gelinas, ONR Workshop on FEL, Sun Valley, ID, June 22-25, 1981.
4. "Diffraction Effects in Free Electron Lasers", J.M. Slater and D.D. Lowenthal, Math Science North West (1980).
5. "Coherent Lienard-Wiechert Fields Produced by FELs", L.R. Elias and J.C. Gallardo, submitted to Physical Rev. for publication; also QIFEL009/81 Report, University of California, Santa Barbara (1981).
6. "Classical Electrodynamics", J.D. Jackson, J. Wiley and Sons (1975).
7. B.M. Kincaid, J. Appl. Phys. 48, 2684 (1977), V. Stagno, G. Brautti, T. Clausen and I. Boscolo, Nuovo Cimento 56, 219 (1980)., H. Motz, J. Appl. Phys. 22, 527 (1951).
8. J.M.J. Madey et al, HEPL Report #819, June 1978.

